

## Subharmonic bifurcation in the sine map: An infinite hierarchy of cusp bistabilities

Mark Schell, Simon Fraser, and Raymond Kapral\*

*Department of Chemistry, University of Toronto, Toronto, Ontario, Canada M5S 1A1,*

(Received 18 March 1983)

The structure of the phase-locked zones in the sine map is examined. Attention is drawn to general features of the map's phase diagram and two, dynamically distinct kinds of bistability are distinguished: One type arises locally through a cusp catastrophe and the other, nonlocally, through crossing (in the parameter plane) of remote stable manifolds. Numerical work indicates that a Cantor set of cusp bistabilities and other related features forms an infinite binary tree in every Arnol'd tongue. (An infinite set of such structures lies arbitrarily close to the parameter line for the quasi-periodic transition to chaos, and also appears in other phase-locked zones.) The binary tree of features obeys the vector scaling found in the quartic map and seems to be generic for multiple-extrema, one-dimensional maps.

### I. INTRODUCTION

Many physical processes involve the entrainment of nonlinear oscillators by a periodic external force. For instance the periodically forced pendulum has served as a paradigm for the study of the complex dynamics exhibited by such systems.<sup>1</sup> Examples arise in the physical and biological sciences: The driven Josephson junction,<sup>2</sup> superionic conductors,<sup>3</sup> and normal and pathological cardiac rhythms<sup>4</sup> are important instances.

The continuous time evolution of these systems is represented by differential equations, but return maps for cross sections of the flow provide equivalent, simplified discrete-time representations of the system's evolution. When strong dissipation is present, the resulting contraction in phase space produces attractors in the map or flow. Injective folding<sup>5</sup> in the domain of the map is an important feature of its dynamics and generates chaotic and diffusive behavior. For example Curry and Yorke<sup>6</sup> have explored the effects of such distortion or breakup of invariant curves in contracting maps of the plane.

It has become commonplace to replace the planar (diffeomorphic) return map by a suitably parametrized, one-dimensional (1D) map. Such 1D maps imitate the behavior of the dominant effective degree of freedom of the system: For a dissipative oscillator this is a phase, but the variable may be interpreted as an underlying periodicity in lattice phenomena.

In this paper we study the sine map

$$x_{t+1} = x_t + a + b \sin(2\pi x_t) \equiv S(x_t; a, b), \quad (1)$$

which is now a widely used model for the nonlinear systems just described.

This map has arisen in a number of contexts and has been studied previously by other investigators. For small  $b$  [ $b < (2\pi)^{-1}$ ] the map is a diffeomorphism and the dynamics (mod 1) have been extensively examined in connection with the properties of mappings of the circumference of a circle onto itself.<sup>7</sup> Very recent works have focused on the universal scaling properties of this map in the region  $b < (2\pi)^{-1} \equiv b_Q$  in connection with the transition from quasiperiodic motion to chaos on an attracting

two-torus.<sup>8</sup> This attractor structure arises from two successive Hopf bifurcations. At incommensurate frequencies the spectrum signals a direct transition to turbulence—like the Ruelle-Takens<sup>9</sup> mechanism. The critical  $b_Q$  value corresponds to incipient folding in the flow.<sup>8</sup> The fine structure of the phase-locking regions of this map for  $b > (2\pi)^{-1}$  has also been investigated recently in a biological context as a model for periodic stimulation of spontaneously beating heart cells.<sup>10</sup> The map dynamics considered on the infinite interval, rather than mod 1, can also model the diffusive behavior of some deterministic, dissipative systems.<sup>11</sup> These latter studies have considered the case where  $a=0$ , but similar considerations apply to the more general case of nonzero  $a$ : The diffusion process is now biased and contains a drift term.

The present paper, which is most closely related to that of Glass and Perez<sup>10</sup> in that it focuses on the fine structure of the phase-locking regions for  $b > (2\pi)^{-1}$ , was stimulated by our recent investigations of hysteresis and bistability phenomena for the cubic map,<sup>12</sup> and by the general features of the subharmonic cascade discovered in the quartic map by Chang, Wortis, and Wright.<sup>13</sup> In some regions of parameter space the local shape of the sine map is similar to that of the cubic map, and one finds the bistabilities characteristic of a map with two extrema. One form of bistability—a cusp-catastrophe phenomenon<sup>12</sup>—is intimately connected with the crossing of superstable lines found in the sine,<sup>10</sup> cubic,<sup>12</sup> and quartic<sup>13</sup> maps, and entails an infinite binary tree of such features.<sup>13</sup>

The purposes of the present paper are, first, to provide an overview of the periodic structure of phase-locked orbits in the sine map by describing features of this structure in both parameter and configuration space; and second, to investigate the binary cascade within the Arnol'd tongues which parallels such structure in the quartic map.<sup>13</sup> Our numerical work indicates the existence of a Cantor set of cusp bistabilities within each tongue showing the vector scaling found for the quartic map.

### II. PHASE DIAGRAM

The general structure of the phase diagram for small  $b$  is well known and consists of phase-locking zones charac-

terized by the rotation number  $\rho$ , whose boundaries are easily computed from perturbation theory.<sup>7</sup> The regions contained within the boundaries corresponding to rational  $\rho$  have a "tongue" shape, while the dynamics corresponding to irrational  $\rho$  occur along lines in the  $(a, b)$  plane. On the  $b=0$  line,  $\rho=a$ , and the regions of rational rotation number are just the set of points with rational  $a$  values; as  $b$  increases, the Arnol'd tongues develop out of these points, and the stable phase-locking solutions occupy regions with finite measure.

The main focus of this study is on the structure of the phase-locking regions for  $b > (2\pi)^{-1}$  where the map possesses extrema which give rise to complex dynamics and bistability. The boundaries of the rational-rotation-number regions correspond to the appearance of a stable periodic orbit by a tangent bifurcation process and, thus, can be computed numerically for general  $b$  values by solving the simultaneous equations

$$S^{(N)}(x; a, b) = x \quad \text{and} \quad S^{(N)'}(x; a, b) = s \quad (2)$$

with slope  $s=1$ . ( $S^{(N)} = S \circ S^{(N-1)}$ , the  $N$ th composition of the map). Within each tongue further pitchfork ( $s=-1$ ) and tangent bifurcations occur for  $b > (2\pi)^{-1}$ . The nature of this fine structure is explored here and in Sec. III. Some idea of the richness of this structure can be obtained by examining Fig. 1, where we see a hierarchy of subharmonic orbits within each Arnol'd tongue—choose the tongue emanating from  $a=0$  for definiteness [Fig. 2(a)]. The region labeled 1 is the stability zone of the fundamental period; where this zone (or a zone corresponding to a subharmonic) crosses other tongues, bistability exits.

The fundamental zones of every tongue are only singly stable, unlike the higher subharmonics. This feature is associated with the (degenerate) cubic superstability at  $b_Q$ , where maximum and minimum superstable lines [ $s=0$ , dashed line labeled  $s_1$  in Fig. 2(a)] meet tangentially. In complete analogy with earlier results for the cubic map,<sup>12</sup> for subharmonic zones the extrema are always distinct and give rise to crossing superstable lines ( $s_2$ ) which are indirectly associated with bistability in such regions. The

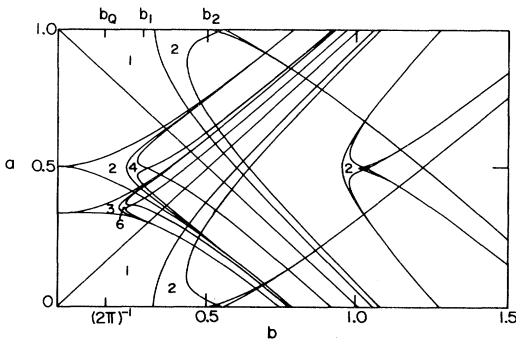


FIG. 1. Phase diagram showing some of the stable phase-locking regions for the sine map. The configurations of crossing harmonic and tangent boundaries within the Arnol'd tongues signal the existence of underlying cusp-catastrophe manifolds. The labels  $b_1 (=0.282)$  and  $b_2 (=0.5)$  are the  $b$  values at which the sections through the solution manifold for the  $a=0, \frac{1}{2}$ , and 1 tongues are shown in Figs. 3 and 4. For  $b > (2\pi)^{-1}$  the map develops extrema.

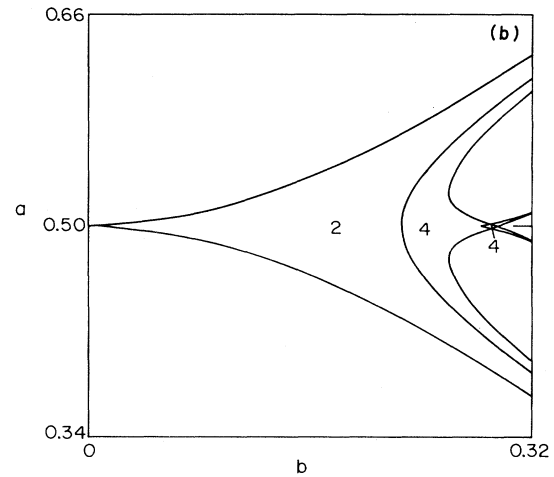
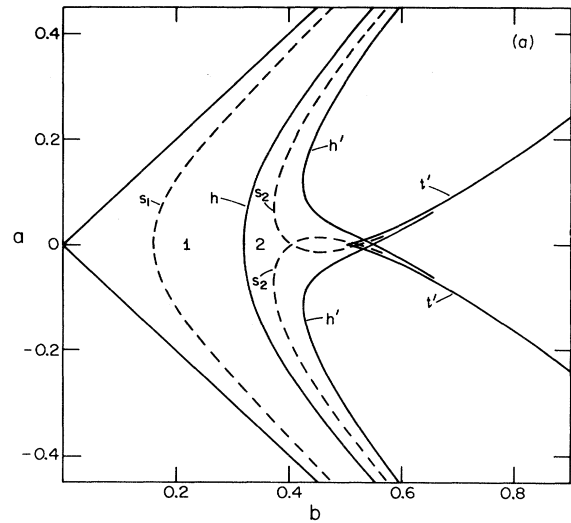


FIG. 2. (a) An enlarged view of the tongue emanating from  $a=0$ . Period 1 is stable in region 1 and superstable along the dashed line  $s_1$ . Period 1 bifurcates to period 2 on  $h$ . Period 2 is stable in region 2 and superstable along the pair of dashed lines  $s_2$ , which cross twice, forming a loop which encloses a cusp at the junction of the tangent boundaries  $t'$ . Period 2 bifurcates to period 4 along lines  $h'$  which cross once to the right of the cusp. (b) An enlarged view of the cusp region in the tongue emanating from  $a = \frac{1}{2}$ . Near the cusp period-4 orbits coexist (cf. Fig. 1).

superstable lines cross twice, forming a loop, at a left doubly superstable point and at a right bistability. This bistability arises from a cusp catastrophe within the loop, and is a local, generic feature for every subharmonic zone. It is quite distinct from the "nonlocal" bistability from crossing tongues, or as we shall see later, from the crossing of subharmonic zones within a tongue. Such cusp-induced bistability also appears in a fundamental zone which arises by tangent bifurcation for  $b > b_Q$  [see, for instance, the period-2 zone near  $(\frac{1}{2}, 1)$  shown in Fig. 1], since in such a zone, again the superstable lines cross rather than merge. Figure 2(b) shows a similar cusp structure in the tongue emanating from  $a = \frac{1}{2}$ .

Further insight into these processes can be gained by examining the manifold structure in  $\{x\} \times \{a, b\}$  space. In Fig. 1 the marks  $b_1$  and  $b_2$  indicate the values at which sections were taken to construct Figs. 3 and 4. In Fig. 3 the manifolds corresponding to the phase-locking zones which originate at  $a=0, \frac{1}{2},$  and 1 are displayed. About the integer  $a$  lines, one has identical sinusoidal manifolds of the period 1 orbits. Part of these manifolds are stable and part unstable, and these portions coalesce at the boundary of the tongue. As  $b$  decreases, the amplitude of the sine wave decreases, and the wave becomes flat at  $b=0$ . The central period-2 manifold is a smaller-amplitude, higher-frequency wave which corresponds to the narrowing of the tongue for higher, periodic, phase-locking zones. All such fundamental manifolds are connected periodic structures in  $x$ , which become flat at  $b=0$  where the sine map has continuous symmetry. The closed loops in Figs. 3 and 4 correspond to the manifolds which arise from the fundamental by a subharmonic process. The antisymmetry of these loops arises from the symmetry properties of the underlying map. The manifold structure in Fig. 3 is derived from the cut through the period-4 cusp at  $a=\frac{1}{2}$ . Thus the period-4 manifolds are tangent to the  $a=\frac{1}{2}$  line at four places; if  $b$  is increased further, the manifolds develop a sigmoidal shape in these regions corresponding to the appearance of a pair of period-4 orbits. Figure 4 shows the development of these manifolds for a larger  $b$  value corresponding to the cusp point, which appears at  $b_2 (= \frac{1}{2})$  along integer  $a$  lines, where the period-2 orbit undergoes orbit doubling. One now sees loops on the sinusoidal period-1 manifolds corresponding to the pitchfork bifurcation to produce period-2, and since  $b$  is set at the cusp point, the period-2 manifolds are tangent to the integer  $a$  lines. Like the period-4 case described above, for  $b$  larger than  $b_2$ , the manifolds develop a sigmoidal shape in these regions when the period-2 orbit-doubling bifurcation occurs. The period-2 and period-4 manifolds about  $a=\frac{1}{2}$  develop further: Clearly the manifolds deform strongly as a result of the increasing amplitude of the fundamental periodic manifolds and their subharmonics as  $b$  increases. The infinity of manifolds corresponding to rational rotation numbers must clearly loop in the  $(x, a, b)$  space in a complicated way in order to avoid crossing.

Another feature of Fig. 4 is worth noting: At this value of  $b$  the period-1 manifolds corresponding to the period-1 orbits  $a=0$  and 1 just touch the line  $a=\frac{1}{2}$ . Hence, at  $(a, b) = (\frac{1}{2}, \frac{1}{2})$ , one manifold has coexisting period-1 orbits, and one manifold is associated with the minimum of the map while the other is associated with the maximum. This is also clear from Fig. 1 where it is seen that the tangent boundaries corresponding to these regions cross. This is just an example of the nonlocal bistability that was briefly mentioned earlier.

We see that the tangent and harmonic boundaries corresponding to phase locking with rational-rotation-number cross in the  $(a, b)$  plane in a complicated way giving rise to bistability: This is precisely the feature that was noted by Glass and Perez<sup>10</sup> in their studies of this system. However, we find that, in addition, each Arnol'd tongue develops an underlying cusp catastrophe manifold for some value of  $b > (2\pi)^{-1}$ . As a result one may observe hysteresis associated with the cusp bistability, and the coexisting orbits may be continuously deformed into one another by mov-

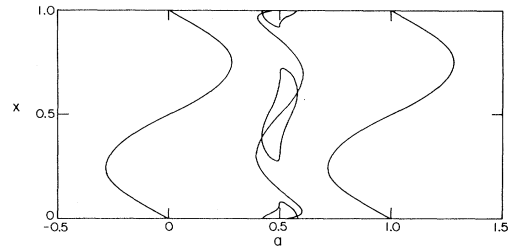


FIG. 3. Manifold structure in  $(x, a)$  space for  $b=b_1=0.282$  corresponding to the tongues emanating from  $a=0, \frac{1}{2},$  and 1. The period-1 manifolds about  $a=0$  and 1 and the period-2 manifold about  $a=\frac{1}{2}$  are shown. These connected manifolds contain both stable and unstable portions. The unconnected period-4 manifold which arises by a pitchfork bifurcation from the period-2 orbit is also shown in the figure. Since the section is taken through the cusp of this subharmonic, the period-4 manifold is tangent to the  $a=\frac{1}{2}$  line in four places.

ing around the cusp: Nonlocal bistability does not possess this feature.

The above description is simply an overall view of the structure of the phase diagram. In fact each Arnol'd tongue develops an infinite hierarchy of cusps which arise from further orbit doublings associated with the subharmonic bifurcation process. The nature and mechanism for the origin of this structure is the subject of the next section.

### III. BINARY-TREE STRUCTURE IN THE TONGUES

In this section we discuss the structural details of the phase diagram within the Arnol'd tongue arising from  $a=b=0$  as shown in Fig. 2(a). Additional numerical work indicates that all the features described here occur in all other tongues, but shrink and approach  $b_Q$  as the order of the phase-locked zone increases [cf. Fig. 2(b)].

The fundamental of this  $a=0$  tongue arises by tangent bifurcation along  $a=\pm b$ . Above the line  $b_Q$  the fundamental bifurcates subharmonically along the hyperbolic boundary  $h$  [see Fig. 2(a)]. All such boundaries have the asymptotic slope  $\pm 1$ . Within the first subharmonic region close to  $b_Q$  there is the cusp bistability mentioned earlier.

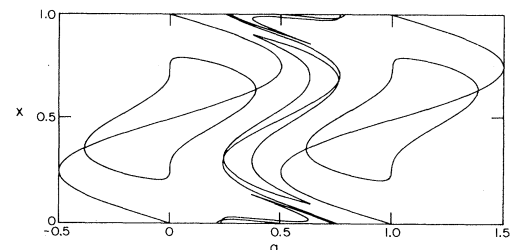


FIG. 4. Manifolds of Fig. 3 are again shown at  $b=b_2=\frac{1}{2}$ . All have widened corresponding to the widening of the tongues as  $b$  increases (cf. Fig. 1). The tongues at  $a=0$  and 1 now have subharmonic manifolds at the cusp catastrophe. The period-4 subharmonic manifold about  $a=\frac{1}{2}$  has folded into a sigmoidal shape. This structure has higher subharmonic loops crossing it (not shown).

An orbit-doubling bifurcation occurs at the cusp, but a tangent bifurcation occurs elsewhere along the lines  $t'$ , meeting at the cusp. The first subharmonic zone has two subharmonic boundaries,  $h'$ , that cross once just to the right of the cusp. In all, the first subharmonic zone has two outer, harmonic processes and two inner, tangent processes, giving it a swallow shape [see Fig. 2(a)]. The superstability lines  $s_2$  within the first subharmonic zone cross twice, once left and once to the right of the cusp. (The left crossing is doubly superstable and the right one locates coexisting superstable orbits.) Thus the subharmonic boundaries  $h'$  move from one superstable line to another in going from an outer, harmonic prong to an inner, tangent prong. In view of this crossing of the lines  $s_2$ , the relation of the structures in the first subharmonic zone to  $h$  implies the duplication of such structure in the second subharmonic zone with respect to  $h'$ : In each of these zones distinct maximum and minimum superstability lines also cross twice enclosing a cusp, and two subharmonic boundaries cross once to the right of the cusp. (Glass and Perez<sup>10</sup> have displayed the period-4 superstable crossings consistent with this feature.) Repetition of this argument implies that with each period doubling, the number of these zones doubles generating (through an infinite binary tree) a Cantor set of cusps (bistabilities) and the associated superstable crossings. The first few features of this tree are shown in Figs. 5(a) and 5(b). The general configuration of superstable crossings has already been observed by Chang, Wortis, and Wright<sup>13</sup>, who showed universal (vector) scaling properties of their structure. Every tongue, however fine, has this Cantor set of features.

Chang *et al.*,<sup>13</sup> point out that the doubly superstable orbits converge (along suitable paths in the tree) to tricritical points, which are also characterized by the accumulation points of cusps, superstable orbits, or indeed other tricritical points. (Tricritical points also lie at one end of Feigenbaum critical lines [i.e., the line limits of subharmonic sequences in the  $(a,b)$  plane] associated with the Cantor set of fine, diagonal processes in the interior of the tongue; see Fig. 5.)

We now outline a method by which an infinity of such tricritical points may be located within an Arnol'd tongue; we have investigated the vector scaling in the  $(a,b)$  plane for a number of such tricritical points.

Consider the solution lines in the  $(a,b)$  plane representing the mapping of the maximum  $M$  of the map into the minimum  $m$  in an odd number of steps and vice versa, that, is the lines such that

$$S^{(j)}(M;a,b)=m, \quad j \text{ odd} \quad (3)$$

and

$$S^{(k)}(m;a,b)=M, \quad k \text{ odd}.$$

We call the first set of lines  $\mathcal{S}_m$  and the second  $\mathcal{S}_M$ . The doubly superstable orbits belong to the intersection  $\mathcal{S}_M \cap \mathcal{S}_m$ , with the additional constraint  $j+k=2^n$  for integer  $n$ . This (intersection) vertex set may be reached along arcs of  $\mathcal{S}_M \cap \mathcal{S}_m$ , so that the union and intersection of  $\mathcal{S}_M$  and  $\mathcal{S}_m$  contain a natural realization of the infinite binary tree ( $\mathcal{B}$ ) of vector-scaling structures. On this tree up ( $u$ ) and down ( $d$ ) are defined as relative direc-

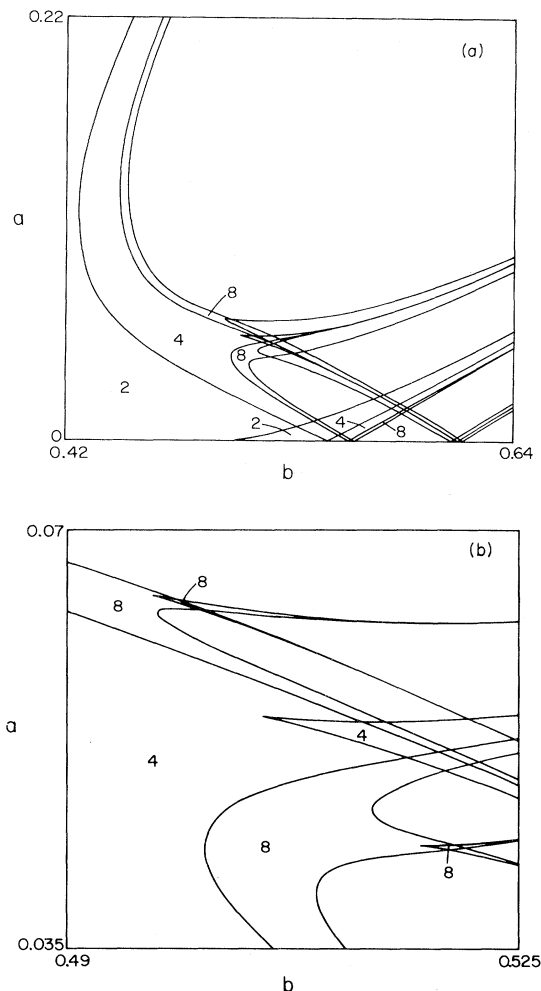


FIG. 5. (a) Detail of the period-2 subharmonic of the  $a=0$  Arnol'd tongue near the cusp. The period-4 zone has a cusp with tangent and crossing subharmonic boundaries. Two period-8 zones appear on either side of the period-4 zone, and so on. (b) Enlargement of the neighborhood of the period-4 cusp. The two period-8 daughters of the period-4 cusp are resolved. Each period-8 cusp has two period-16 cusps (not shown), etc.

tions to the last step taken in the direction of increasing period. We show some of the lines of  $\mathcal{S}_M \cup \mathcal{S}_m$  in Fig. 6.

In Fig. 6 we can easily see, starting from the period-4 doubly superstable orbit, that we may move  $u$  or  $d$  in the  $(a,b)$  plane to a period-8 orbit; from either of these period-8 orbits we may move  $u$  or  $d$  to a period-16 orbit on  $\mathcal{B}$ . In fact the situation is geometrically rather simple: From any doubly superstable orbit an  $u^\infty$  or  $d^\infty$  walk always lies along a smooth, relatively straight curve—a stem in  $\mathcal{S}_M$  or  $\mathcal{S}_m$ . Whatever the first finite number of steps taken on  $\mathcal{B}$ , the scaling approaching a tricritical point along a stem is  $\delta_T^{(1)}=7.284\dots$ , which as has been pointed out,<sup>13</sup> is Feigenbaum's<sup>14</sup> quartic exponent. We have also verified, for a number of walks, that eventually, side-branch structure at  $ud, u^2d, u^3d, \dots, u^\infty d$ , for example, scales with the second "odd-perturbation" exponent found

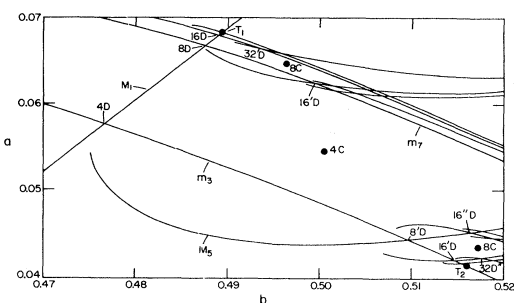


FIG. 6. Graph of curves  $M_k$  and  $m_j$  for odd  $j$ , where  $S_M \equiv \{M_j\}$  and  $S_m \equiv \{m_j\}$  (see text).  $M_j$  crosses  $m_k$  at a doubly superstable orbit (D). A subharmonic exists for  $j+k=2^n$  (integer  $n$ ). Along stem  $M_1$  intersections with  $m_k$  (at 4D, 8D, 16D, etc.) scale with exponent  $\delta_T^{(1)}=7.284\dots$  and accumulate at  $T_1$ . With respect to  $M_1$  the (subharmonic) side-branch points 8'D, 16'D (upper), 32'D, etc., scale with exponent  $\delta_T^{(2)}=2.857\dots$ . Along (stem)  $m_3$  from 4D, 8'D, 16'D (lower), etc., scale with  $\delta_T^{(1)}$  reaching the tricritical point  $T_2$ . Again side-branch points 16''D, 32''D, etc., scale with exponent  $\delta_T^{(2)}$  accumulating at  $T_2$ . The cusps 4C, two 8C's, etc., scale with exponent  $\delta_T^{(2)}$  with respect to the appropriate stem.

by Chang *et al.*,<sup>13</sup> for the quartic map,  $\delta_T^{(2)}=2.857\dots$ . All the side branches are eventually parallel near the tricritical point  $T_1$  which is reached by a  $u^\infty$  walk. Globally on  $\mathcal{B}$  this second exponent governs side-branch scaling with respect to a chosen stem or any other stem's "lateral" features like cusps, other side-branch points in the vertex set, and indeed their tricritical limits. The eigenvectors for the scaling directions about a given  $T$  are defined by the stem leading to  $T$  ( $\sim\delta_T^{(1)}$ ) and side branches ( $\sim\delta_T^{(2)}$ ). [The eigenvectors in this instance refer to structures in the  $(a, b)$  plane.] Figure 7 is a schematic representation of the above features.

From the structure of the phase diagram we see that it is always possible to reach the fundamental periodic zone from a remote tricritical point along a stem, but these regions do not obey Feigenbaum (scalar) scaling with exponent  $\delta_F=4.669\dots$ , but rather they obey two-exponent vector scaling for the stem part of the walk. For such a remote tricritical point the nearest bands of subharmonic cascade with  $\delta_F$  scaling start at some (high) subharmonic.<sup>13</sup> Far into the tree hierarchy, the lowest subharmonic of such a sequence becomes arbitrarily high, and the number of such sequences and their associated tricritical points increases as  $2^n$ . These sequences are just the diagonal processes referred to earlier in Fig. 5(a).

Although there appears to be very strong evidence for Change *et al.*,<sup>13</sup> vector scaling ubiquitously in  $\mathcal{B}$  for stem walks, the associated eigenvectors change in absolute and relative orientation: In any neighborhood of a tricritical point, the angle between a stem and its branches increases with the number of branch turnings on the walks. In the limit of an infinity of such turnings, this angle seems to approach  $180^\circ$ . Thus any scaling feature in the neighborhood of a tricritical point  $T$  has embedded in it other similar, smaller, skewed scaling features arising from the infinity of possible side turnings in the tree traversals near  $T$ . Some features of these secondary and/or higher substructures are, under an affine transformation, self-similar

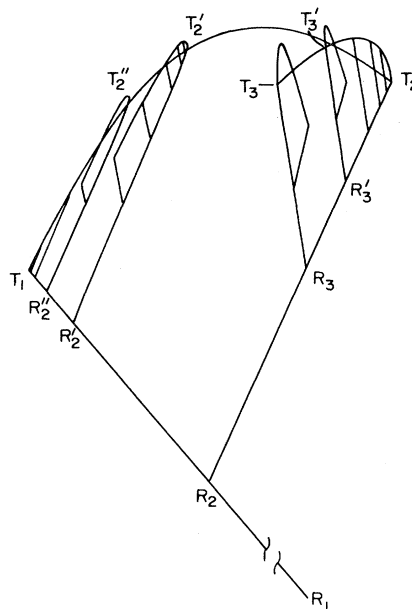


FIG. 7. Schematic representation of the tree of doubly superstable orbits (vertices) of Fig. 6. From vertex  $R_1$  successive vertices  $R_2, R_2', R_2'', \dots$ , scale with exponent  $\delta_T^{(1)}$  accumulating at the (primary) tricritical point  $T_1$ , and side-branch structure relative to  $R_1 T_1$  scales with exponent  $\delta_T^{(2)}$ , e.g., the distance from  $R_1 T_1$  to the secondary tricritical points  $T_2, T_2', T_2'', \dots$ , accumulating at  $T_1$ .  $T_2$  is the limit of vertices  $R_3, R_3', R_3'', \dots$ , scaling with  $\delta_T^{(1)}$  along  $R_2 T_2$ . Tertiary tricritical points  $T_3, T_3', T_3'', \dots$ , accumulating at  $T_2$  are shown. The angles  $R_1 \hat{R}_2 T_2, R_2 \hat{R}_3 T_3, \dots$ , increase with the number of side turnings at the roots  $R_2, R_3, \dots$ . Any  $T$  has an infinity of  $T$ 's in its neighborhood.

to the primary structure near  $T$ . The neighborhood of every  $T$  contains Cantor-point sets arising from this structural hierarchy. These features are illustrated schematically in Fig. 7. The local coalescence of eigenvectors implicit in the proposed limiting angle behavior appears to be evident in *udud*, *dudu*, etc. walks. Limiting colinearity of the  $\delta_T^{(1)}$  and  $\delta_T^{(2)}$  eigenvectors implies singular behavior.

#### IV. CONCLUSION

The sine map has become important recently since it is a model showing<sup>8</sup> a universal quasiperiodic transition to turbulence. In this paper we have drawn attention to general features of the periodic zones of this map's phase diagram and to an infinite hierarchy of bifurcations within these periodic zones. This feature apparently always occurs within any subharmonic progression in the sine map. The configuration of superstable lines corresponding to this structure has also been observed by Glass and Belair.<sup>15</sup> Two further cases, the cubic map and the quartic map, also exhibit the same phenomenon, and it seems to be generic for multiple-extrema, one-dimensional maps. Within the higher-order Arnol'd tongues of the sine map, the entire binary-tree structure lies arbitrarily close to the parameter line for the quasiperiodic transition to chaos, and may therefore have experimental relevance to the "neighboring" chaotic phenomena.

Chang, Wortis, and Wright<sup>13</sup> discovered vector scaling in the tree structure for the quartic map; we have demonstrated the existence of their scaling about a number of tricritical limit points terminating walks on the tree, and conjecture that is obeyed at an infinity of such points. This scaling is most easily followed on the set of doubly superstable orbits, at crossings of superstable lines; associated "bistable" crossings also appear on these lines—an important additional dynamical feature embedded in the tree is bistability arising locally from a cusp catastrophe (this feature is intimately connected with the two kinds of superstable crossing).

The tree structure is a vector generalization of Feigenbaum's one-parameter scaling and suggests that general one-dimensional—map models and the dissipative planar maps and flows, which they are intended to imitate, will show similar dynamical variety.

#### ACKNOWLEDGMENT

This research was supported in part by a grant from the Natural Sciences and Engineering Research Council of Canada.

\*On sabbatical leave at Service de Chimie Physique II, Université Libre, B-1050 Brussels, Belgium (1982–1983).

<sup>1</sup>See, for example, B. V. Chirikov, *Phys. Rep.* **52**, 263 (1979).

<sup>2</sup>B. A. Huberman, J. P. Crutchfield, and N. H. Packard, *Appl. Phys. Lett.* **37**, 750 (1980).

<sup>3</sup>*Physics of Superionic Conductors*, edited by M. B. Salamon (Springer, New York, 1979).

<sup>4</sup>M. R. Guevara and L. Glass, *J. Math. Biol.* **14**, 1 (1982); A. T. Winfree, *The Geometry of Biological Time* (Springer, New York, 1980).

<sup>5</sup>See the account of the "horseshoe" by S. Smale, *The Mathematics of Time* (Springer, New York, 1980); P. Couillet, C. Tresser, and A. Arneodo, *Phys. Lett.* **77A**, 327 (1980).

<sup>6</sup>J. H. Curry and J. A. Yorke, in *The Structure of Attractors in Dynamical Systems*, Vol. 668 of *Lecture Notes in Mathematics*, edited by N. G. Markley, J. C. Martin, and W. Perrizo (Springer, New York, 1977).

<sup>7</sup>A. Denjoy, *J. Math Pures Appl.* **11**, 333 (1932); V. I. Arnol'd, *Izv. Akad. Nauk, SSSR, Ser. Mat.* **25**, 21 (1961) [Transl. Amer. Math. Soc. **46**, 213 (1965)]; M. Herman, in *Geometry*

and *Topology*, Vol. 597 of *Lecture Notes in Mathematics*, edited by J. Palis (Springer, Berlin, 1977).

<sup>8</sup>D. Rand, S. Ostlund, J. Sethna, and E. Siggia, *Phys. Rev. Lett.* **49**, 132 (1982); M. J. Feigenbaum, L. P. Kadanoff, and S. J. Shenker, *Physica* **5D**, 370 (1982); S. J. Shenker, *ibid.* **5D**, 405 (1982).

<sup>9</sup>D. Ruelle and F. Takens, *Commun. Math. Phys.* **20**, 167 (1971).

<sup>10</sup>L. Glass and R. Perez, *Phys. Rev. Lett.* **48**, 1772 (1982); R. Perez and L. Glass, *Phys. Lett.* **90A**, 441 (1982); L. Glass, M. Guevara, A. Shrier, and R. Perez, *Physica D* (in press).

<sup>11</sup>T. Geisel and J. Nierwetberg, *Phys. Rev. Lett.* **48**, 7 (1982); M. Schell, S. Fraser, and R. Kapral, *Phys. Rev. A* **26**, 504 (1982); S. Grossmann and H. Fujisaka, *ibid.* **26**, 1779 (1982).

<sup>12</sup>S. Fraser and R. Kapral, *Phys. Rev. A* **25**, 3223 (1982); S. Fraser, E. Celarier, and R. Kapral, *J. Stat. Phys.* (in press).

<sup>13</sup>S.-J. Chang, M. Wortis, and J. Wright, *Phys. Rev. A* **24**, 2669 (1981).

<sup>14</sup>M. J. Feigenbaum, *J. Stat. Phys.* **19**, 25 (1978); **21**, 669 (1979).

<sup>15</sup>L. Glass and J. Belair (unpublished).